# On Signaling Power: Communications over Wireless Energy

Raul G. Cid-Fuentes*, M. Yousof Naderi†, Stefano Basagni†,
Kaushik R. Chowdhury†, Albert Cabellos-Aparicio* and Eduard Alarcón*,
*NaNoNetworking Center in Catalunya (N3Cat), Universitat Politècnica de Catalunya, Spain
†Electrical and Computer Engineering Department, Northeastern University, USA
Email: rgomez@ac.upc.edu, naderi@coe.neu.edu, basagni@ece.neu.edu,
krc@ece.neu.edu, acabello@ac.upc.edu, eduard.alarcon@upc.edu

***Abstract*—Wireless RF power transmission from dedicated Energy Transmitters (ETs) is emerging as a promising approach to enable battery-less wireless networked sensor systems. However, when data communication and RF energy recharging occur in-band, sharing the RF medium and devoting separate access times for both operations raises architectural and protocol level challenges. This paper proposes a novel method of concurrent transmission of data and energy to solve this problem, allowing ETs to transmit energy and sensors to transmit data in the same band synchronously. Our key idea concerns devising a physical layer modulation scheme that allows the data transmitting node to introduce variations in the envelope of the energy signal at the intended recipient. We implemented a proof-of-concept receiver, modeled and validated through extensive experimentation. We then propose a new physical layer mechanism for guaranteed successful delivery of information in a point-to-point link. Quantitative results demonstrate the feasibility of joint energy-data transfer, along with its associated benefits and tradeoffs.**

## I. Introduction

Wireless networked sensing systems are the "invisible" enablers of pervasive communications and the Internet of Things. A notable example in this field refers to graphene nano-antennas that are enabling the Internet of nano-Things as an increasingly essential part of our everyday life [1]. Powering these systems is becoming the crucial challenge, as key requirements such as cost effectiveness, very small form factors and decade-long lifetimes are difficult to meet by using nodes that are battery-less or with low-capacity batteries.

A recently investigated viable approach to power and/or recharge these systems concerns the use of dedicated Energy Transmitters (ETs) that send RF power to the system nodes wirelessly [2]. This technique aims at leveraging RF energy harvesting, allowing controlled powering of nodes that may have insufficient residual energy in their batteries, or that are unable to scavenge ambient energy at desired rates. Using the RF spectrum for both energy and data transfer, however, may seriously affect network operations and performance, and require sophisticated hardware and devices that many systems cannot afford. For instance, transmitting energy and data on different frequencies [3] would require multiple or broadband access capabilities, since the frequency gap between energy and data communications cannot be very small [4]. Alternatively, when both energy and data share a single band, specialized MAC protocols are required [5]. In both cases, devices should feature two separate RF front-ends, for decoding the information and converting RF energy into DC [6]. Therefore, devising methods for energy provisioning without affecting data communications appears to be the challenge to tackle [7]. For instance, transmission of both point-to-point energy and data enables downlink communications from a base station (BS) to a node [8]. This is also beneficial in terms of hardware costs, since the signal receiver can be integrated in the energy harvester [9]. For uplink communications full duplex techniques have been proposed where the BS is able to simultaneously transmit energy and receive information on the same frequency [10]. However, enabling communication among network nodes while an ET is transmitting power still needs to be investigated [11].

In this paper, we propose a new method for concurrent in band transmission of data and energy, where nodes exchange data among each other while being re-charged by ETs at the same time. The combined signal at the antenna of the receiving node is characterized by a large bias component (generated by the transmission of energy) with small fluctuations (caused by the overlapping data). In order to enable successful data reception we decode the information by using the built-in energy detection properties of energy harvesters. This detection intermodulates both data and energy signals, amplifying the data signal through the action of the ET as a remote data signal amplifier. Then, a novel physical layer technique is designed to mitigate the data and energy phase misalignment.

The main contributions of this paper are as follow.

- We present a communication model for data reception through energy harvesters, providing insights on the treatment of the signal through the action of the energy harvester.
- We validate this model by testbed-based experiments using off-the-shelf hardware, showing the simultaneous recharging of a node as it efficiently decodes data signals through its energy harvester.
- We develop a new physical layer technique to mitigate the obstacles that our approach brings towards guaranteeing a successful point-to-point packet delivery.

The rest of the paper is so organized. In Section II we describe the fundamentals of our Communications over wire-

less Energy (CoE) scheme. Section III presents a communication model for the energy harvester. In Section IV we experimentally validate the proposed communication model. In Section V we describe a physical layer to enable reliable point-to-point communications. The corresponding link is evaluated in Section VI. Related works are reviewed in Section VII. Finally, Section VIII concludes the paper.

## II. Communications over Wireless Energy

This section defines our Communications over wireless Energy (CoE) scheme and describes the network topology that enables it.

### A. Overview

We consider an RF wireless powered point-to-point link, made up of three components: An energy transmitter (ET), a transmitting node, and a receiving node. The purpose of the ET is to transmit power to the nodes. The nodes implement CoE to communicate between them.

The key idea of CoE is that of overlapping the simultaneous transmissions of data and energy in such a way that both transmissions can be successfully recovered at the receiving node. To do this, the transmitting node superimposes a low-power RF signal that modulates the envelope of the energy transmission, basically using the ET as a remote data signal amplifier (RDSA). The energy transmission is expectedly orders of magnitude larger than the power of the data transmission. To obviate this imbalance, the receiving node opportunistically utilizes the nonlinear properties of its energy harvester to intermodulate both transmissions, extract the data signal and retain the harvested energy.

This approach brings several benefits to the node. First, it reduces system complexity, as the node can be equipped with only one antenna and a single RF front-end for both data and energy reception. Second, the action of the ET as RDSA removes the need for an internal RF amplifier.Third, it enables low-power coherent signal reception without power hungry components (e.g., RF mixers). Finally, given that data and energy transmissions are simultaneous, the complexity of the MAC layer is reduced.

### B. Design of a CoE transceiver

Designing a CoE device requires addressing two major challenges. First, the power required to implement CoE operation should be as low as possible, to enable energy neutral operations. Second, devices must be able to tolerate differences of orders of magnitude between the power of the simultaneous data and energy transmissions.

Fig. 1 shows the block diagram of a device with CoE. Since the transmitter and the energy harvester both use the same RF frequency, they are connected to the same antenna. The harvester is in charge of converting the RF energy into electric current to power the sensor, as well as of acting as an RF front-end for signal reception. (The communication data path in reception is showed in gray.)

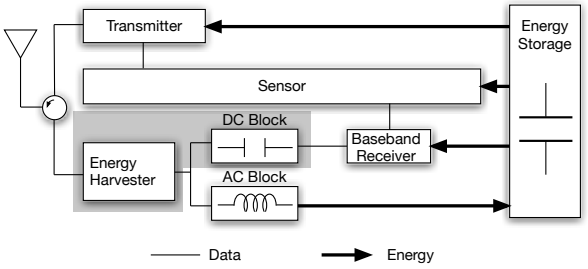


Fig. 1. A CoE node.

*Transmitter architecture*. The design of the transmitter is not particularly challenging, and state-of-the-art wireless transmitters can be used to transmit data to the receiving sensor, since signal overlapping is performed at the antenna of the receiving node. Each transmitting node (i.e., the ET and a node) just generates an RF wave that is wirelessly propagated to the destination antenna.

*Receiver architecture*. Designing a CoE data receiver is challenging since the RF waves overlap at the receiving antenna. Therefore, this antenna must be able to separate the two transmissions, and do it with as little power as possible. To address these challenges we use an energy harvester as both data and energy receiver. The idea is that of leveraging the energy transmission to amplify the data transmission, thus eliminating the need of power hungry signal amplifiers and performing a coherent RF baseband downconversion where oscillators are no longer required (Section III-A).

## III. Energy Harvesters as Data Receivers

In this section we describe a communication model for energy harvesters that are used as signal receivers for CoE, where the signal is recovered by sensing the output current of the energy harvester. The aim of this model is to help understanding why the energy harvester is suitable for data reception. Our model divides the action of an energy harvester as a signal receiver into conventional communication blocks and provides a high-level explanation of the reception process. The model is shown in Fig. 2.

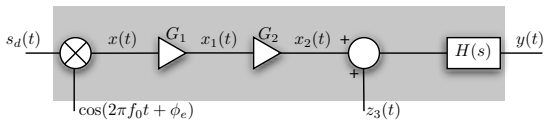


Fig. 2. Communication model of a CoE energy harvester as a signal receiver.

It is made up of five components: A 1D homodyne receiver, two amplifier stages ($G_1$ and $G_2$), additive noise and an output low-pass filter.

### A. Extracting the low-power overlapped information

The input power detection of an energy harvester used as a signal receiver for CoE implements the following two communication blocks.

- A 1D Homodyne receiver. The received RF signal is converted to baseband. Given that this unit is one-dimensional, only data arriving at the receiver in-phase with the energy transmission is received.
- An amplifying stage of gain $G_1 = 2\sqrt{\frac{P_e}{P_d}}$, where $P_e$ and $P_d$ are the received power from the energy and data transmissions, respectively.

The energy harvester operates as a power processing circuit that converts the available power received by the antenna into an electrical current, so that an energy storage unit can be recharged. Unlike signal processing circuits, power processing circuits maintain the relation between input and output power, determined by a certain efficiency. By assuming a fixed antenna impedance and a fixed output voltage, we observed that its output current is proportional to its input power. Therefore: $I_{out} = \beta V_{in}^2$, where $\beta$ is a constant that depends on the electrical properties of the energy harvester (among others, its input-to-output power conversion efficiency), the input impedance of the circuit and the impedance matching. The RMS value of the generated voltage at the antenna $V_{in}$ is such that $P_{in} = V_{in}^2/R_a$, with $R_a$ being the antenna impedance.

At the receiving node, both energy and data signals are received simultaneously. First, the transmitted data signal arrives at the receiving end as:

$$s_d(t) = \sqrt{2P_d}\left[b_I(t)\cos\left(2\pi f_0 t + \phi_d\right) - b_Q \sin\left(2\pi f_0 t + \phi_d\right)\right] \quad (1)$$

where $P_d$ is power received from the data signal, $f_0$ is the carrier frequency, and $\phi_d$ is the phase shift of the data at the receiving node. The phase and quadrature components of the baseband data stream, $b_I$ and $b_Q$, are such that $E[B] = E[b_I + jb_Q] = 0$ and $E[|B|^2] = 1$, where $E[\cdot]$ is the statistical expectation. Then, the transmitted energy, characterized as a large power carrier wave, arrives at the receiver node as:

$$s_e(t) = \sqrt{2P_e}\cos(2\pi f_0 t + \phi_e), \quad (2)$$

where $P_e$ is the received power from the energy signal and $f_0$ stands for the carrier frequency. Notice that the carrier frequency of both transmissions are the same.

The energy harvester performs power detection, which is transferred to the output in form of current. The input power can be calculated as:

$$x_1(t) = \left|s_d(t) + s_e(t) + z_1(t)\right|^2, \quad (3)$$

where $z_1(t)$ is the additive white Gaussian noise (AWGN) generated at the receiving antenna, with power $P_{N1}$. By substituting $s_d$ and $s_e$ from equations (1) and (2), respectively, neglecting the high-frequency terms (i.e., the terms at frequency $2f_0$), and assuming $P_e \gg P_d$, we can approximate Equation (3) by:

$$x_1(t) = P_e + 2\sqrt{P_d P_e}\,\Re\left\{B(t)e^{\phi}\right\} + z_2(t), \quad (4)$$

where $P_e$ is the data signal received power, $B$ indicates the modulated information, $\phi$ is the phase shift between the energy and data transmissions, and $z_2(t)$ is the noise at the output of the energy harvester due to the antenna noise, defined as $z_2(t) = 2\sqrt{P_e P_{N1}}\,\Re\left\{z_1 e^{j\phi_e}\right\}$.

Counter-intuitively, decoding data during the transmission of energy shows significant benefits, as it performs a coherent reception and because the dual action of the ET as RDSA amplifies the data signal.

### *B. Power-to-current (P-I) gain*

The detected signal is converted into small variations of the electrical current generated by the energy harvester. Even though, this conversion is ideally linear, it has been experimentally observed that the efficiency of the energy harvester is input-power dependent [12]. In general, we find that the output current is characterized by the power to current transconductance $g$, and it can be written as:

$$I_0 + x_2 = g(P_e + x_1(t)),$$

where $I_0$ is the constant component of the output current of the energy harvester and $x_2$ refers to its small signal fluctuations (Fig. 2). To derive the small signal gain, we approximate this function by its first order Taylor polynomial:

$$I_0 + x_2 \approx g(P_e) + \frac{\partial g}{\partial P}(P_e)x_1,$$

where $\frac{\partial g}{\partial P}(P_e)$ is the derivative of $g(\cdot)$ with respect to the input power evaluated in $P_e$. As a result, the P-I gain $G_2$ is:

$$G_2 = \frac{\partial g}{\partial P}(P_e). \quad (5)$$

Fig. 3 plots the gain $G_2$ (Equation (5)) for the Powerharvester P1100 from Powercast Co. [13].

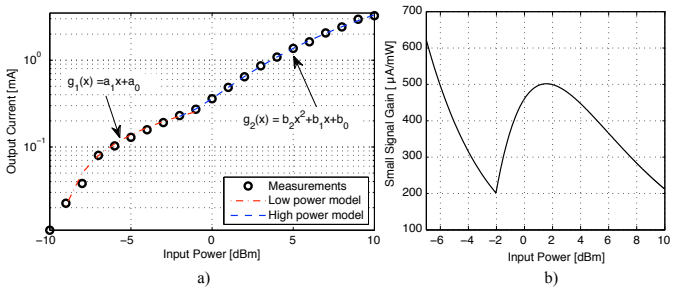


Fig. 3. (a) Characterization of the output current of the Powerharvester P1100 [13]. (b) Calculation of its small signal gain $G_2$.

To obtain this curve, we have first measured its input power to output current relation (Fig. 3 (a)). The output DC current is modeled by a piece-wise function, with two distinguishable regions of operation. At input powers $< -1$dBm the output current, as a function of the input power (in dBm), can be modeled with the first order polynomial $g_1(x)$. At high input power it can be modeled by a second order polynomial $g_2(x)$:

$$g_1(x) = 2.935x + 0.2843 \text{ [mA/dBm]}.$$
$$g_2(x) = 1.912x^2 + 0.1058x + 0.3607 \text{ [mA/dBm]}.$$

We then calculate $G_2$ as the partial derivative of the obtained piece-wise function with respect to the input power (Fig. 3 (b)). Notice that this must be calculated in linear units, instead of dBm. We observe that the gain $G_2$ depends on the input power of the energy signal and it ranges from 200 $\mu$A/mW to 600 $\mu$A/mW.

### C. Additive noise

As the noise that an energy harvester generates depends on the circuit topology, devices and design, it is not possible to provide a generic closed-form expression. As a consequence, the estimation of these values has to be performed either at circuit design time or by experimentation. Notice that current energy harvesters do not target signal processing applications, and therefore, these are not optimized for low-noise. We expect that custom circuit design for CoE applications will lower the overall noise. According to our experiments (Section IV), we have measured a combined energy harvesting and measurement system noise characterized as AWGN with spectral density of -80 dBmA/Hz.

We refer as $Z_3$ to the overall induced noise of the system, this is given by:

$$Z_3 = Z_{EH} + G_2 Z_2,$$

where $Z_{EH}$ is the internal noise, and $G_2 Z_2$ represents the contribution of the antenna noise after the P-I conversion stage.

### D. Output filter

As the main purpose of energy harvesters is to regulate the output voltage, their circuits contain a relatively large output equivalent capacitance to provide a stable output. Unfortunately, this parallel capacitance at the output of the energy harvester limits the bandwidth of the output current, hence limiting the maximum achievable bit rate. To model this last output stage, we find that the effective output current of an energy harvester is low-pass filtered by:

$$H(s) = \frac{Z_0}{Z_0 + Z_{sense}},$$

with $Z_0$ being the output impedance and $Z_{sense}$ is the associated input impedance to the current sensing and energy storage unit. According to our experiments, the output impedance of a Powerharvester P1100 from Powercast Co. [13] is capacitive with capacitance $C_L = 5.5$ $\mu$F. Then, we have utilized a resistor as $Z_{sense}$ to sense variations in the output current, which has ranged between 1 $\Omega$ and 100 $\Omega$.

In this case, the output filter becomes a first order low-pass filter, given by:

$$H(s) = \frac{\tau}{s + \tau},$$

where $\tau = R_{sense} C_L$. In our experiments, the cut-off frequency of the output ranges from 11.4 kHz (using $R_{sense} = 1$ $\Omega$) to 1.14 MHz (when $R_{sense} = 100$ $\Omega$).

### E. Decoding the symbol

Once the signal is extracted, a baseband receiver must decode signal levels into a binary stream. We consider two main decoding alternatives.

*Comparator-based decoding*. By employing a comparator-based decoder, the received signal is compared against a given threshold, thus providing only two logic values. This is the most basic implementation of a signal receiver and shows significant advantages in power saving (offering a power consumption $< 1$ $\mu$W as reported in the literature [14]). However, these circuits suffer from low-performance, since no advanced signal processing techniques can be implemented.

*ADC-based decoding*. As a more advanced technique to recover information, the receiving sensor can implement analog-to-digital converters. This option requires a significantly larger amount of energy but enables the use of more advanced signal processing tools to improve signal quality. Power consumption in state-of-the-art micro power ADC in the order of a few tens of $\mu$W have been reported [15].

## IV. Proof of Concept

In this section we develop a CoE receiver using off-the-shelf hardware, and evaluate the model from Section III and its performance.

### A. Implementation design and experimental set-up

Our experimental set-up is shown in Fig. 4.

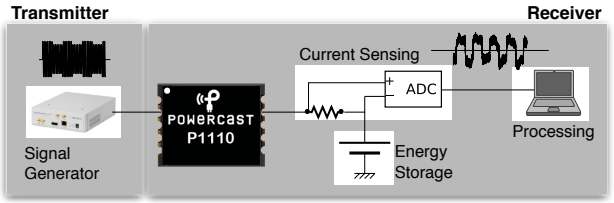


Fig. 4. Experimental set-up.

*Transmitter set-up*. We used a signal generator that generates both energy and data transmissions at a fixed frequency of 915 MHz. The energy transmission is composed of a sine wave with power ranging from -1 dBm to 4 dBm. We have also implemented a BPSK modulation at a rate of 1 kbps for data transmission. The power of the data signal is in the range from -68 dBm to -48 dBm.

*Receiver set-up*. We base our signal and energy receiver on off-the-shelf energy harvester Powerharvester P1100 from Powercast [13]. This circuit offers a reasonable performance in the desired frequency band, with efficiency rates above 50% for input powers ranging from -5 dBm to 20 dBm. The output current as a function of the input power is shown in Fig. 3 (a).

The output of the energy harvester has been connected to a super-capacitor operating as energy storage and management unit of the overall circuit. This unit is in charge of providing continuous operation over time, and its design presents several trade-offs [16]. Given that we are not constrained by the size of the circuits, in this paper we have employed a capacity

of 220 mF to ensure a steady output voltage during data reception.

A series resistor has been employed to sense the output current of the energy harvester. These resistors provide outstanding current sensing performance due to their linear properties. Given that the sensing gain is related to the resistance value, larger values provide a larger gain. However, resistors increase power losses and increase noise. Through experimentation, we have observed that values between 1 Ω to 100 Ω offer a reasonable tradeoff between sensing gain and power losses. In Fig. 5 we show the power losses associated with using different resistor at different input power levels, and compare it to the harvested power considering a Powerharvester P1100 [13]. In addition, we show the ideal operation of an energy harvester (i.e., output power equaling input power, dashed line).

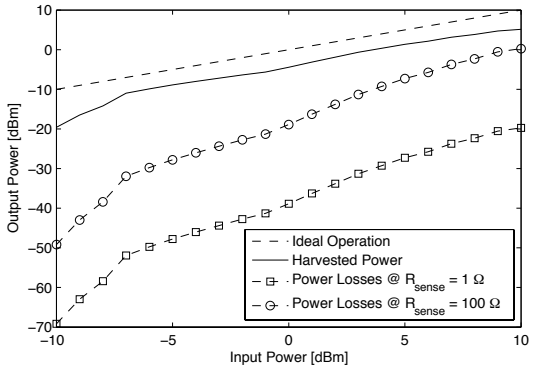


Fig. 5. Power losses with different resistors vs. ideal operations.

*Signal decoding*. We have implemented a software-defined, computer based signal receiver. In particular, we have implemented a 16 bit analog-to-digital converter (ADC) with a sampling frequency of 10 kHz. The combination of the sensing resistor with the ADC provides a signal gain of $G_3 = 1310$ mV/mA units. We expect baseband signal decoders for sensors used for low-power applications to be of much lower performance and probably implementing comparator-based schemes. Once digitized, a matched filter is implemented and the optimum sampling time is computed. Finally, the decision threshold is computed to perform signal detection, so that the bit error rate (BER) is minimized. Accordingly, this last communication block converts the sensed voltages into a binary stream.

### B. Evaluation

To evaluate the validity and performance of this approach, we first perform proof-of-concept measurements. Then, we validate the communication model by observing the type of RF-to-baseband conversion and its gain. Finally, we evaluate the receiver performance as a function of the bit error rate (BER), by assuming a null phase shift between energy and data transmissions.

*Proof of concept*. We first validate the key idea that an energy harvester has built-in properties as a CoE signal receiver. Specifically, we measure the voltage drop at the current sensing resistor to detect the transmission of binary data. We set up a transmission of energy with a power of $P_e = 2$ dBm at a fixed frequency of 915 MHz. Overlapped to this RF wave, we transmit a periodic binary sequence, using a BPSK modulation with power $P_d = -49$ dBm and bit rate of 130 bps at the same center frequency of 915 MHz. This periodic binary sequence emulates actual data transmission.

Fig. 6 depicts the sensed voltage drop at the resistor.

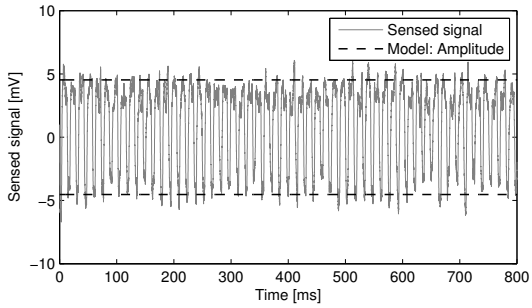


Fig. 6. Recovered signal from an energy harvester used as data receiver.

The binary sequence can be recovered, showing two distinguishable voltage levels centered at 0 mV and with a voltage difference of approximately 8 mV (i.e., approximately 4 mV signal amplitude). This signal is compared to the expected sensed voltage according to the communication model (Section IV-B). In addition, we observe a certain ripple in the voltage levels of approximately 2 mV, which is a combination of the antenna, energy harvester and sensing noise.

*Model validation*. In Fig. 7 we show the sensed peak-to-peak voltage at the input of the signal decoding unit. We observe the operation of the ET as RDSA, since the sensed voltage is effectively modulated by the received input power. In Fig. 8 we compare the sensed peak-to-peak voltage to the expected value according to our model. Our observation shows that the model is effective in predicting the sensed value with great accuracy in case for power $P_e = 1$ dBm. We also observe that as this power grows, there appears a noticeable mismatch among the values. This is due to the fact that the small-signal approximation no longer applies for large values. Nonetheless, the value provided by the model is still within the same order of magnitude, thus still being useful for link budget calculations.

*Calculation of the BER*. We next evaluate the performance of the receiver for CoE. In particular, we measure the bit error rate (BER) observed when transmitting a raw binary sequence encoded in a BPSK modulation at a bit rate of 1 kbps. Given that a $BER < 10^{-2}$ can be considered enough in the context of device-to-device communications (when considering packet sizes of around 100 bits and implementing simple repetition coding [14]), we consider a $BER = 10^{-2}$ as our target. Additionally, we will refer as receiver sensitivity (in power units) as the minimum power that is required in order to obtain the targeted BER.

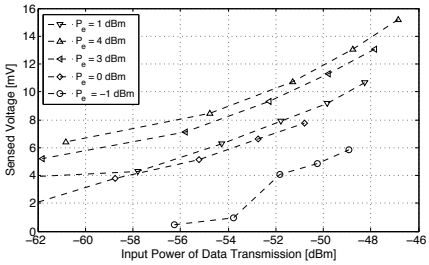


Fig. 7. Peak-to-peak voltage difference at the input of the signal decoder as a function of the input power of both data and energy transmissions.

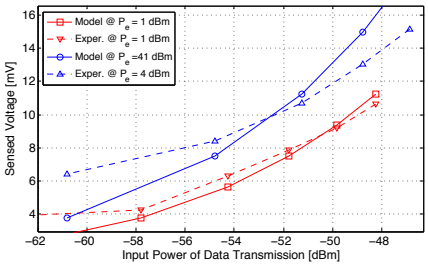


Fig. 8. Model validation for the peak-to-peak voltage difference at the input of the signal decoder.

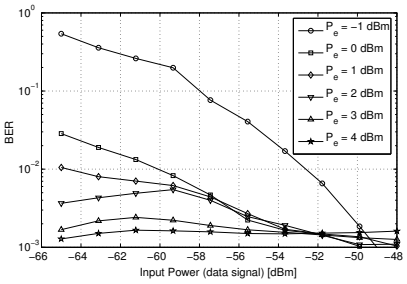


Fig. 9. BER as a function of the input power of the data signal.

Fig. 9 shows the BER as a function of the power of the data transmission, for different values of power in the overlapped transmission of data and energy. In our experimental setup, we have obtained BERs confined around $10^{-3}$. This has two main reasons: 1) The appearance of flicker noise in our current sensing platform, and 2) the lack of implemented delay-locked loop components to overcome temporal drifts. Implementing a signal amplification stage before the ADC unit can significantly improve the signal quality at the cost of higher power consumption. As shown by the figure, the intermodulation between energy and data plays a key role in the performance of the device. Particularly, we observe that sensitivities of -53 dBm are required if the device is harvesting a power of $P_e = -1$ dBm, whereas this is reduced down to -65 dBm if the harvested power is increased just by 2 dB. The achieved performance using off-the-shelf hardware proves the feasibility of this approach and motivates further research in joint energy-data hardware design.

## V. Physical Layer Design

In this section, we devise a physical layer for CoE, which aims to guarantee that the transmitted information can be successfully decoded at the destination node. The main aim of this layer is to handle the phase shift misalignment between the received transmissions of data and energy through time-multiplexing techniques.

### A. Time-multiplexing coherent reception

The properties as 1D homodyne receiver of an energy harvester enables coherent reception using power-saving, and even power generating, components. However, given that the phase shift between data and energy transmissions cannot be controlled, there appears a distinct possibility that the modulated transmission cannot be received.

Implementing simple retransmissions of data packets can improve the eventual packet error rate (PER). We show in Fig. 10 the cumulative distribution function (CDF) of the packet error rate, when a data packet is being retransmitted assuming two different retransmission policies, namely reassigning a random phase shift and retransmitting the packet with a phase shift of $\pi/2$.

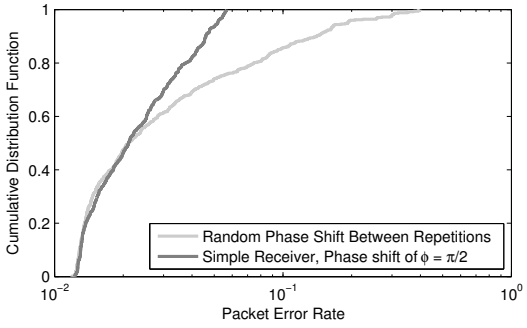


Fig. 10. CDF of the PER for simple retransmissions of data packets.

Although this approach can achieve relatively low PER values, this solution renders inefficient in terms of energy consumption. For this, we implement a time-multiplexed coherent reception. To implement this concept, each symbol transmission is divided into two time epochs, namely $e_I$ and $e_Q$. Both time epochs contain the same symbol, but with a phase shift of $\pi/2$ rad. In phasor notation, the transmitted symbol during the time epochs can be written as $s_I = b = b_I + jb_Q$ and $s_Q = -jb = b_Q - jb_I$. This approach lets the receiver to project the received symbol into two orthogonal axis. By assuming a generic phase shift between data and energy, $\phi$, the received symbol at each epoch is given by:

$$\hat{s}_I = \Re\left\{s_I e^{\phi}\right\} = b_I \cos(\phi) - b_Q \sin(\phi) \tag{6}$$

$$\hat{s}_Q = \Re\left\{s_Q e^{\phi}\right\} = b_Q \cos(\phi) + b_I \sin(\phi). \tag{7}$$

Then, by estimating this phase misalignment, the transmitted symbol can be successfully recovered. For this, the received symbol must be multiplied by the rotation matrix, $\hat{b} = \mathbf{R}\hat{s}$, the rotation matrix is defined as:

$$\mathbf{R} = \begin{bmatrix} \cos(\hat{\phi}) & -\sin(\hat{\phi}) \\ \sin(\hat{\phi}) & \cos(\hat{\phi}) \end{bmatrix} \tag{8}$$

where $\hat{\phi}$ refers to the estimated phase shift. An error in the phase estimation $\epsilon = \hat{\phi} - \phi$ will eventually impact upon the received symbol by:

$$\hat{b} = \begin{bmatrix} b_I \cos(\epsilon) - b_Q \sin(\epsilon) \\ b_Q \cos(\epsilon) + b_I \sin(\epsilon) \end{bmatrix} \quad (9)$$

We next show the separated implementation of the physical layer at both the transmitting and receiving ends.

### B. Transmitter

Fig. 11 illustrates the block diagram of the operation of the transmitter node implementing time-multiplexed coherent transmission.

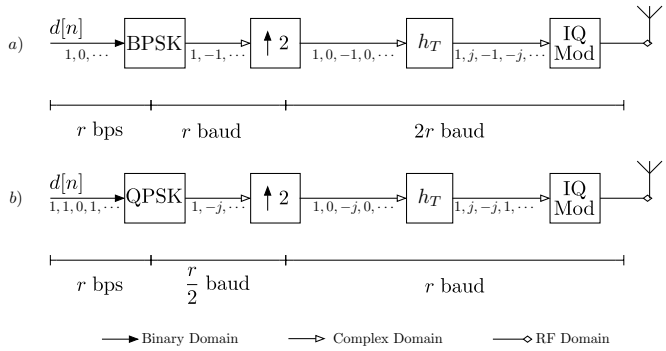


Fig. 11. PHY-Layer of the transmitter. (a) BPSK modulation and (b) QPSK modulation.

The transmitter encodes the bit stream $d[n]$ at a rate of $r$ bits per second into either a BPSK (Fig. 11 (a)) or a QPSK (Fig. 11 (b)) signal at a rate of $r$ or $r/2$ symbols per second, respectively. Then, the signal is interpolated by two, such that samples are placed between zeros. Afterwards, the signal is convoluted with the interpolator filter $h_T$, defined as:

$$h_T = \begin{bmatrix} 1 \\ -j \end{bmatrix}.$$

Finally, the signal is IQ modulated and transferred to the antenna. By employing this physical layer, we time multiplex the two dimensions of a coherence transmission (i.e., the I-Q components). Using one or the other modulation will depend on the receiving capabilities of the destination node.

### C. Receiver

A block diagram of the operations of the receiver node is shown in Fig. 12.

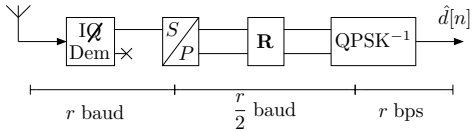


Fig. 12. PHY-Layer of the receiver for both BPSK and QPSK modulations (QPSK case).

The received signal first passes through a 1D homodyne demodulator, represented as the IQ dem block.. This unit represents the action of the energy harvester as a signal receiver, which is able to only collect the projection of the data signal over the phase of the energy signal). Provided that the Q component is transmitted through time-multiplexing, the I component is passed through a 1-input-2-output serial-parallel to emulate the reception of both components. This signal is then multiplied by the aforementioned matrix $\mathbf{R}$ which is used to correct the phase shift between the energy and data signals.

### D. Packet framing and data-energy phase-shift estimation

A physical layer header is considered in the transmission of each data packet. This header must include a known binary sequence used to perform the estimation of the channel state information (CSI) at the receiver (i.e., the matrix $\mathbf{R}$). In particular, the data-energy phase shift is estimated by calculating the scalar product between the known sequence and the received signal.

## VI. Physical Layer Evaluation

We emulate the proposed physical layer for data and energy phase misalignment mitigation using MATLAB software and evaluate its performance. For this, we first evaluate the BER as a function of the ratio between the energy per bit and the noise level, $E_b/N_0$. This is a standard metric that allows us to better compare the performance of our approach against conventional receivers.

To derive the BER calculations, we evaluate the model, i.e., equations from (6) to (9) with modulations BPSK and QPSK, considering both comparator or ADC based receivers. To derive generic results, we have considered generic AWGN antenna noise (the internal noise of the receiver has not been considered).

### A. Comparator-based receiver

Given that simple communication schemes based on energy detection can only recover non-coherent amplitude shift keying (ASK) modulations, we compare in Fig. 13 the BER as a function of the $E_b/N_0$ with a preamble of 4, 8 and 16 bits and compare the obtained results to the BER of theoretical non-coherent ASK [17]. In addition, we also show the obtained BER if the proposed physical layer is not implemented and the theoretical BER for coherent ASK [17].

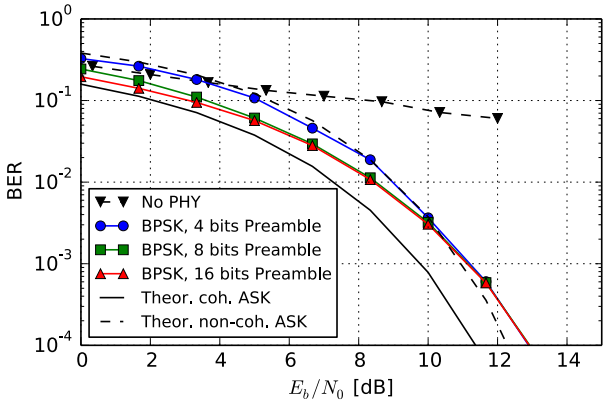


Fig. 13. Comparison of the obtained BER between a comparator-based receiver for CoE and classical communication schemes.

It is first observed that CoE requires a physical layer to operate well. Then, we find that CoE outperforms in terms of BER non-coherent detection for values of $E_b/N_0$ below 10.5 dB. In addition, we find that CoE improves the sensitivity of our system (fixing a threshold of $BER < 10^{-2}$) by 0.6 dB. Finally, we observe that the obtained BER is lower bounded by the theoretical coherent ASK reception.

### B. ADC-based receiver

Analog-to-digital converters can offer higher accuracy and performance during the signal detection process at the cost of higher power consumption. By using this approach, we can leverage signal processing techniques and to use CSI estimation techniques to correct the phase shift between the data and the energy signal. We find that on the one hand, we can transmit information using QPSK modulations (i.e., we can double the achievable throughput of a sensor node), as well as to approach the theoretical limit in BER as a function of the $E_b/N_0$ ratio.

We show in Fig. 14 the obtained BER as a function of the $E_b/N_0$ ratio for BPSK and QPSK modulations. In the figure, we compare the performance as a function of the number of quantization bits employed in the ADC. In addition, we show the theoretical bound for BPSK and QPSK, as well as the coherent ASK bound in the BER.

We observe that the BPSK modulation is more robust to a low number of quantization bits than QPSK. We also note that this curve approaches the theoretical bound for coherent ASK when the number of quantization bits becomes sufficiently large. That is, there is a loss of 3 dB compared to ideal BPSK due to the fact that each symbol is transmitted twice using the time-multiplexed I and Q components. However, given that this approach enables low-power coherent detection through the energy detection mechanism of an energy harvester, this performance is still remarkable and better than non-coherent energy detection mechanisms.

Alternatively, we see that QPSK shows less resilience to a low number quantization bits. Nonetheless, we observe that the set of QPSK curves approaches the theoretical bound for BPSK and QPSK when the number of quantization bits becomes sufficiently large. That is, the proposed physical layer overcomes the phase misalignment between data and energy transmissions, and permits a near optimal operation if an ADC-based CoE receiver is implemented.

## VII. Related Works

Simultaneous wireless information and power transfer (SWIPT) and full duplex energy harvesting have been presented in [8], [10]. These technologies aim to deliver information over a wireless medium during the simultaneous transmission of energy. However, SWIPT enables the transmission of data and energy from the same network device, thus enabling downlink communications, whereas full-duplex energy harvesting aims at receiving energy as the device transmits it, thus targeting uplink communications. In these fields, significant work has been recently performed, which includes

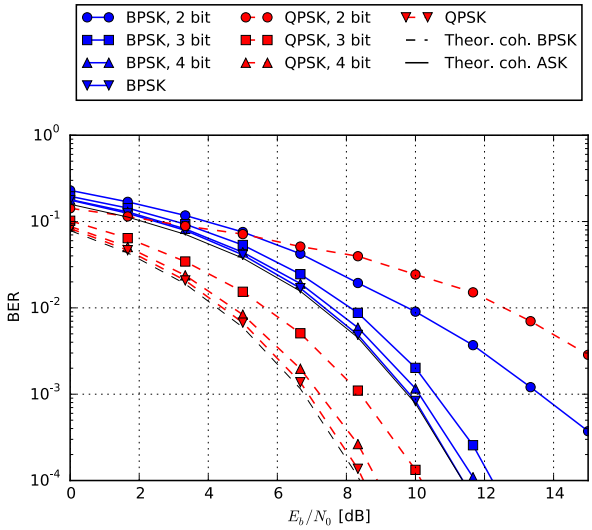


Fig. 14. Comparison of the obtained BER between a comparator-based receiver for CoE and classical communication schemes.

considering MIMO-based solutions [18] or simultaneous relay of energy and data [19]. In particular, a model for integrated data and energy transmission using SWIPT has been presented in [9].

We contextualize CoE with other simultaneous data and energy transmission technologies in Fig. 15.

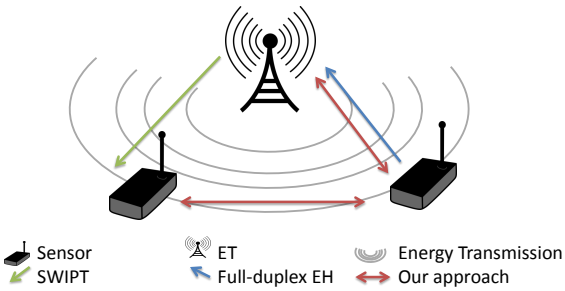


Fig. 15. CoE vs. existing simultaneous data and energy transmission technologies.

In particular, we compare our CoE approach to SWIPT [8] and full-duplex EH [10]. These three approaches show potential to operate together within a single network.

Simultaneous transmission of energy and data is also provided by other technologies. For instance, RFID technologies inherently implement simultaneous transmission of energy and data, being based on backscatter communications [20]. In line with this approach, backscatter communications have recently been presented and experimentally demonstrated for wireless RF [14]. This approach leverages ambient RF waves produced by a third entity that are passively reflected from the transmitting to the receiving node. To reflect the RF wave and to modulate information, the impedance of the antenna is being constantly modified at the transmitter (i.e., short-circuiting and open circuiting the antenna to modify its reflec-

tion properties and to transmit logic '1's and '0's). Ambient backscatter enables ultra low power communications over an active transmission of energy. However, the transmitting node cannot allocate power as it reflects a portion of the power that it receives, whereas the allocated power in our approach is a design parameter. On the receiver side, no integrated data and energy receiver has been implemented, so the receiving sensor has to switch between activities, thus requiring synchronized MAC protocols to detect active data transmission.

## VIII. Conclusions

This paper introduces Communications over wireless Energy (CoE) as a method to enable simultaneous energy and data transfer for the wireless networked systems such as Internet of Things. We show that transmission of in-time, in-band data and energy permits uninterrupted transmission of energy, as well as a reduction of system design redundancy. To accomplish the successful reception of data, energy transmitters (ETs) have shown a key role to enhance the signal quality at the receiver, which decodes the information through its energy harvester. To validate this approach, we have modeled and implemented a proof-of-concept receiver, which has been validated through extensive experimentation. A physical layer is proposed to mitigate the energy and data phase misalignment. We provided quantitative results to demonstrate the viability of our joint energy and data transfer approach, offering sensitivity below -60 dBm with off-the-shelf energy harvesters. Our results open the door to the design of future joint energy and data RF harvesters.

## Acknowledgments

This work has been partially funded by the Spanish State "Ministry of Economy and Competitiveness" under grant aid PCIN-2015-012, "Ministry of Science and Innovation" under grant aid DPI2013-47799-C2-2-R and in part by the US National Science Foundation under research grant CNS-1452628.

## References

[1] I. Llatser, C. Kremers, A. Cabellos-Aparicio, J. M. Jornet, E. Alarcn, and D. N. Chigrin, "Graphene-based nano-patch antenna for terahertz radiation," *Photonics and Nanostructures - Fundamentals and Applications*, vol. 10, no. 4, pp. 353–358, 2012, taCoNa-Photonics 2011.

[2] Z. Popovic, E. Falkenstein, D. Costinett, and R. Zane, "Low-power far-field wireless powering for wireless sensors," *Proceedings of the IEEE*, vol. 101, no. 6, pp. 1397–1409, June 2013.

[3] H. Nishimoto, Y. Kawahara, and T. Asami, "Prototype implementation of ambient RF energy harvesting wireless sensor networks," in *IEEE Sensors*, November 2010, pp. 1282–1287.

[4] M. Y. Naderi, K. R. Chowdhury, S. Basagni, W. Heinzelman, S. De, and S. Jana, "Surviving wireless energy interference in RF-harvesting sensor networks: An empirical study," in *Proceeding of IEEE SECON—Workshop on Energy Harvesting Communications*, June 2014.

[5] M. Y. Naderi, P. Nintanavongsa, and K. R. Chowdhury, "RF-MAC: A medium access control protocol for re-chargeable sensor networks powered by wireless energy harvesting," *IEEE Transactions on Wireless Communications*, vol. 13, no. 7, pp. 3926–3937, 2014.

[6] A. N. Parks, A. Liu, S. Gollakota, and J. R. Smith, "Turbocharging ambient backscatter communication," in *Proceedings of ACM SIGCOMM*, Chicago, IL, 2014, pp. 619–630.

[7] P. Grover and A. Sahai, "Shannon meets Tesla: Wireless information and power transfer," in *Proceeding of IEEE ISIT*, June 2010, pp. 2363–2367.

[8] L. Liu, R. Zhang, and K. C. Chua, "Wireless information transfer with opportunistic energy harvesting," *IEEE Transactions on Wireless Communications*, vol. 12, no. 1, pp. 288–300, January 2013.

[9] X. Zhou, R. Zhang, and C. K. Ho, "Wireless information and power transfer: Architecture design and rate-energy tradeoff," *IEEE Transactions on Communications*, vol. 61, no. 11, pp. 4757–4767, November 2013.

[10] X. Kang, C. K. Ho, and S. Sun, "Full-duplex wireless-powered communication network with energy causality," *IEEE Transactions on Wireless Communications*, vol. 14, no. 10, pp. 5539–5551, October 2015.

[11] L. Xiao, P. Wang, D. Niyato, D. Kim, and Z. Han, "Wireless networks with RF energy harvesting: A contemporary survey," *IEEE Communications Surveys & Tutorials*, vol. 17, no. 2, pp. 757–789, 2015.

[12] R. G. Cid-Fuentes, M. Y. Naderi, K. R. Chowdhury, E. Alarcon, and A. Cabellos-Aparicio, "Leveraging deliberately generated interferences for multi-sensor wireless RF power transmission," in *Proceedings of IEEE Globecom*, December 6–10 2015.

[13] Powercast Corporation, "P1110–915 MHz RF Powerharvester Receiver." [Online]. Available: http://www.powercastco.com/PDF/P1110-datasheet.pdf

[14] V. Liu, A. Parks, V. Talla, S. Gollakota, D. Wetherall, and J. R. Smith, "Ambient backscatter: Wireless communication out of thin air," *SIGCOMM Comput. Commun. Rev.*, vol. 43, no. 4, pp. 39–50, Aug. 2013.

[15] N. Verma and A. P. Chandrakasan, "An ultra low energy 12-bit rate-resolution scalable SAR ADC for wireless sensor nodes," *IEEE Journal of Solid-State Circuits*, vol. 42, no. 6, pp. 1196–1205, June 2007.

[16] R. G. Cid-Fuentes, A. Cabellos-Aparicio, and E. Alarcon, "Energy buffer dimensioning through Energy-Erlangs in spatio-temporal-correlated energy-harvesting-enabled wireless sensor networks," *IEEE Journal on Emerging and Selected Topics in Circuits and Systems*, vol. 4, no. 3, pp. 301–312, September 2014.

[17] Y. Kim, S.-W. Tam, G.-S. Byun, H. Wu, L. Nan, G. Reinman, J. Cong, and M.-C. Chang, "Analysis of noncoherent ASK modulation-based RF-interconnect for memory interface," *IEEE Journal on Emerging and Selected Topics in Circuits and Systems*, vol. 2, no. 2, pp. 200–209, June 2012.

[18] R. Zhang and C. K. Ho, "MIMO broadcasting for simultaneous wireless information and power transfer," *IEEE Transactions on Wireless Communications*, vol. 12, no. 5, pp. 1989–2001, May 2013.

[19] Z. Chen, B. Xia, and H. Liu, "Wireless information and power transfer in two-way amplify-and-forward relaying channels," in *Proceedings of IEEE GlobalSIP*, December 3–5 2014, pp. 168–172.

[20] R. Want, "An introduction to RFID technology," *IEEE Pervasive Computing*, vol. 5, no. 1, pp. 25–33, January 2006.